ISSN 2350-1022

International Journal of Recent Research in Mathematics Computer Science and Information Technology
Vol. 11, Issue 2, pp: (84-91), Month: October 2024 – March 2025, Available at: www.paperpublications.org

Analysis of Riga plates and Magnetism inclination effects on Temperature profile for unsteady MHD Stokes flow of a dusty fluid

[1]Opiyo Richard Otieno, [2]Oroni M. Juma

[1,2] Dept of Pure & Applied Mathematics, Maseno University (Kenya) December 30, 2024

DOI: https://doi.org/10.5281/zenodo.14950208

Published Date: 01-March-2025

Abstract: **The effect of inclined Riga plates and dust particle concentration on the temperature of an unsteady MHD Stokes flow of a dusty fluid was examined. The flow equations were derived and solved via explicit finite difference method following a similarity transformation. Simulations revealed that as the inclination angle of the Riga plates (η) approaches 90^0, the temperatures of both fluid and dust particles increase. Additionally, an increase in dust particles' concen- tration leads to a rise in flow temperature.**

***Keywords*: MHD, Dusty fluid, inclined angle, Riga plate, Magnetism.**

1. INTRODUCTION

A fluid containing small inert particles, typically disregarded in analysis, is referred to as a dusty fluid when these particles are also considered. In viscous flow, the presence of dusty particles is highly significant in industries such as petroleum and crude oil refinement. The mathematical theory of fluid flow through a porous medium was pioneered by Darcy [5]. From there henceforth, scientific and computational research on flows followed on. Ismail et al [5] investigated the unsteady Stokes flow of a dusty fluid between two parallel plates through a porous medium, with constant suction applied to the upper plate and injection to the lower plate. As per the study's assumptions, the findings revealed that dust particles had a higher velocity compared to the fluid velocity. They did not analyze the temperature profiles of the individual components of the flow. Additionally, the plates were neither Riga plates nor inclined. A Riga plate is a flat surface that consists of electrodes and permanent magnets arranged in alternating manner to create a uniform polarity and magnetization. These plates generate electromagnetic forces when an electric current passes through them, which can influence the temperature, velocity and direction of fluid flow. Islam et al. [3] investigated micropolar fluid flow along an inclined Riga plate through a porous medium. Their study concluded that varying the inclination angle did not result in temperature changes. Igbal et al [2], explored an electrically conducting Riga plate in viscous nanofluid flow considering viscous dissipation, thermal radiation, and melting heat and proposed stagnation point flow over the Riga plate. Heat and mass transfer in MHD flow was explored by Onyinkwa et al[7] and Otieno et al [8]. In [7], It was established that The maximum temperature profile is obtained at an inclination angle. In [8], as the angle of inclination of magnetic field increases, the temperature of the flow also increases. Nasrin et al. [4] investigated dusty fluid flow between two parallel Riga plates within a porous medium, but they provided limited discussion on the impact of dust particle concentration and inclined plates on the flow's temperature. This identified gaps served as the foundation for the current study.

2. PROBLEM FORMULATION

Consider a flow of a dusty fluid between parallel Riga plates, which are inclined at an angle η from the horizontal plane. These plates are stationary and maintained at constant but distinct temperatures. The fluid is assumed to be viscous and incompressible, flowing along the x-axis, while the y-axis is perpendicular to the flow direction. The fluid flow is driven by a pressure gradient p. The presence of Riga plates induces a uniform magnetic force on the fluid. The following is a sketch of the physical concept of the problem.

ISSN 2350-1022

International Journal of Recent Research in Mathematics Computer Science and Information Technology
Vol. 11, Issue 2, pp: (84-91), Month: October 2024 – March 2025, Available at: www.paperpublications.org

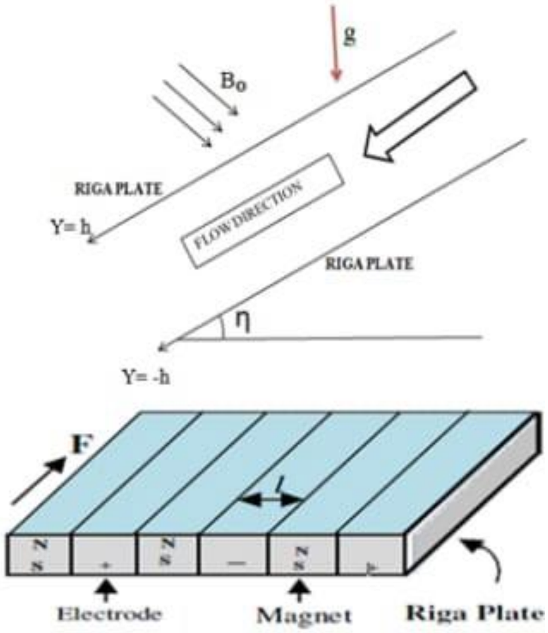

Figure 2.1: Geometry of the physical problem

Where; g is the force of gravity, B_o is the inclined magnetic field and η is the angle of inclination of the Riga plates. The boundary conditions for the flow are;

$$u = 0, u_d = 0, T = 0, T_d = 0,\ at\ y = -h \tag{2.0.1}$$

$$u = 0, u_d = 0, T = 1, T_d = 1, at\ y = h$$

Subject to figure 2.1 and equation (2.0.2) the developed temperature and momentum governing equations are;

$$\frac{\partial T}{\partial t} = \frac{k_c}{\rho C_p}\left(\frac{\partial^2 T}{\partial y^2}\right) + \frac{v}{C_p}\left(\frac{\partial u}{\partial y}\right)^2 - \frac{2k_c K_s N_d}{3\rho^2 v C_p}(T - T_d) + \frac{u\sigma}{\rho C_p}\overrightarrow{B_0^2}\, sin^2\gamma \tag{2.0.2}$$

$$\frac{\partial T_d}{\partial t} = \frac{2k_c K_s N_d}{3\rho v \rho_m C_s}(T - T_d) \tag{2.0.3}$$

$$\frac{\partial u}{\partial t} = -\frac{1}{\rho}\frac{\partial p}{\partial x} + v\frac{\partial^2 u}{\partial y^2} + \frac{\pi J_0 M_0}{8\rho}e^{\frac{-y\pi}{l}} + g\sin\eta - \frac{u\,\sigma}{\rho}\overrightarrow{B_0^2}\, sin^2\gamma - \frac{vu}{k_*} - \frac{1}{\rho}K_s N_d(u - u_d) \tag{2.0.4}$$

$$m_d\frac{\partial u_d}{\partial t} = K_s N_d(u - u_d) \tag{2.0.5}$$

where; u is the velocity of the fluid particle, p is the pressure of the flow, J_o is the current concentration/density in the Riga plates electrodes. M_o is the magnetic field effect created by the alternating permanent magnets on Riga plate and l is the distance between the electrodes, which is the width of the magnets, ρ is the density of the fluid, electrical conductivity feature of the fluid is σ, γ is the angle of inclination of the magnetic field, K_s is the Stokes constant, N_d is the number of dust particles per unit volume, m_d is the mass of dust particles, $\nu = \frac{\mu}{\rho}$ and δ is the electrical conductivity.

2.0.1 Non-Dimensionalisation of the governing equation

The main objective of Non-dimensionalisation is to set the solutions obtained in situation of a given set of conditions to be applicable to a geometrically similar environment but experiencing totally different conditions. The following parameters are used to non-dimensionalise the governing equations.

$$\hat{x} = \frac{\pi}{l}x,\ \hat{y} = \frac{\pi}{l}y, \hat{u} = \frac{l}{\pi v}u, \widehat{u_d} = \frac{l}{\pi v}u_d$$

$$\hat{p} = \frac{l^2 p}{\pi^2\rho v^2}, \hat{t} = \frac{\pi^2 v}{l^2}t, \Theta = \frac{T - T_1}{T_2 - T_1}, \Theta_d = \frac{T_d - T_1}{T_2 - T_1} \tag{2.0.6}$$

ISSN 2350-1022

International Journal of Recent Research in Mathematics Computer Science and Information Technology
Vol. 11, Issue 2, pp: (84-91), Month: October 2024 – March 2025, Available at: www.paperpublications.org

The non-dimensionalisation of temperature equation terms for fluid and dust particles is as below

$$\frac{\partial T}{\partial t} = \frac{\partial T}{\partial \Theta} \cdot \frac{\partial \Theta}{\partial \hat{t}} \cdot \frac{\partial \hat{t}}{\partial \Theta} = \frac{\pi^2 v (T_2 - T_1)}{l^2} \frac{\partial \Theta}{\partial \hat{t}} \quad (2.0.7)$$

$$\frac{\partial T}{\partial y} = \frac{\partial T}{\partial \Theta} \cdot \frac{\partial \hat{y}}{\partial y} \cdot \frac{\partial \Theta}{\partial \hat{y}} = \frac{\pi (T_2 - T_1)}{l} \frac{\partial \Theta}{\partial \hat{y}} \quad (2.0.8)$$

$$\frac{\partial^2 T}{\partial y^2} = \frac{\partial}{\partial \hat{y}} \left(\frac{\partial T}{\partial y}\right) \frac{\partial \hat{y}}{\partial y} = \frac{\partial}{\partial \hat{y}} \left[\frac{(T_2 - T_1)\pi}{l} \frac{\partial \Theta}{\partial \hat{y}}\right] \frac{\pi}{l} = \frac{\pi^2 v (T_2 - T_1)}{l^2} \frac{\partial^2 \Theta}{\partial \hat{y}^2} \quad (2.0.9)$$

$$\frac{\partial T_d}{\partial t} = \frac{\partial T_d}{\partial \Theta_d} \cdot \frac{\partial \hat{t}}{\partial t} \cdot \frac{\partial \Theta_d}{\partial \hat{t}} = (T_2 - T_1) . \frac{\pi^2 v}{l^2} . \frac{\partial \Theta_d}{\partial \hat{t}} \quad (2.0.10)$$

$$\frac{\partial u}{\partial t} = \frac{\partial u}{\partial \hat{u}} \cdot \frac{\partial \hat{t}}{\partial t} \cdot \frac{\partial \hat{u}}{\partial \hat{t}} = \frac{\pi v}{l} \cdot \frac{\pi^2 v}{l^2} \cdot \frac{\partial \hat{u}}{\partial \hat{t}} = \frac{\pi^3 v}{l^3} \frac{\partial \hat{u}}{\partial \hat{t}} \quad (2.0.11)$$

$$\frac{\partial p}{\partial x} = \frac{\partial p}{\partial \hat{p}} \cdot \frac{\partial \hat{x}}{\partial x} \cdot \frac{\partial \hat{p}}{\partial \hat{x}} = \frac{\pi^2 \rho v^2}{l^2} \cdot \frac{\pi}{l} \cdot \frac{\partial \hat{p}}{\partial \hat{x}} = \frac{\pi^3 \rho v^2}{l^3} \frac{\partial \hat{p}}{\partial \hat{x}} \quad (2.0.12)$$

$$\frac{\partial u}{\partial y} = \frac{\partial u}{\partial \hat{u}} \cdot \frac{\partial \hat{y}}{\partial y} \cdot \frac{\partial \hat{u}}{\partial \hat{y}} = \frac{\pi v}{l} \cdot \frac{\pi}{l} \cdot \frac{\partial \hat{u}}{\partial \hat{y}} = \frac{\pi^2 v}{l^2} \frac{\partial \hat{u}}{\partial \hat{y}} \quad (2.0.13)$$

$$\frac{\partial^2 u}{\partial y^2} = \frac{\partial}{\partial y} \left(\frac{\partial u}{\partial y}\right) = \frac{\partial}{\partial \hat{y}} \left(\frac{\pi^2 v}{l^2} \frac{\partial \hat{u}}{\partial \hat{y}}\right) \frac{\partial \hat{y}}{\partial y} = \frac{\partial}{\partial \hat{y}} \left(\frac{\pi^2 v}{l^2} \frac{\partial \hat{u}}{\partial \hat{y}}\right) \frac{\pi}{l}$$

$$\frac{\partial^2 u}{\partial y^2} = \frac{\pi^3 v}{l^3} \frac{\partial^2 u}{\partial \hat{y}^2}$$

Substituting equation (2.0.7 - 2.0.9) into equation (2.0.2), equation (2.0.10) into equation (2.0.3) and since $(T - T_d) = (\Theta - \Theta_d)(T_2 - T_1)$ then dividing the equations through by $\frac{\pi^2 v (T_2 - T_1)}{l^2}$ to obtain;

$$\frac{\partial \Theta}{\partial \hat{t}} = \frac{k_c}{\rho C_p} \left(\frac{1}{v}\right) \left(\frac{\partial^2 \Theta}{\partial \hat{y}^2}\right) + \frac{v}{C_p (T_2 - T_1)} \left(\frac{\partial \hat{u}}{\partial \hat{y}}\right)^2 + \frac{2 l^2 k_c K_s N_d}{3 \rho^2 v^2 \pi^2 C_p} (\Theta - \Theta_d) + \frac{\hat{u} l^2 \sigma B_0^2 \sin^2 \gamma}{\rho v C_p \pi^2 (T_2 - T_1)} \quad (2.0.14)$$

$$\frac{\partial \Theta_d}{\partial \hat{t}} = \frac{2 k_c K_s N_d l^2 (\Theta - \Theta_d)}{3 \rho \rho_m c_s \pi^2 v^2} \quad (2.0.15)$$

$$\frac{\partial \hat{u}}{\partial \hat{t}} = -\frac{\partial \hat{p}}{\partial \hat{x}} + \frac{v}{v} \frac{\partial^2 \hat{u}}{\partial \hat{y}^2} + \frac{l^3 J_0 M_0}{\pi^2 v^2 8 \rho} e^{-y} + \frac{l^3 g}{\pi^3 v^2} \sin \eta - \frac{l^3 \hat{u} \sigma B_0^2 \sin^2 \gamma}{\pi^2 v^2 \rho} - \frac{v l^3 \hat{u}}{k_* \pi^2 v^2} - \frac{l^3 K_s N_d}{\pi^2 v^2 \rho} (\hat{u} - \hat{u}_d) \quad (2.0.16)$$

$$\frac{\partial \hat{u}_d}{\partial \hat{t}} = \frac{l^3 K_s N_d}{v^2 \pi^3 m_d} (\hat{u} - \hat{u}_d) \quad (2.0.17)$$

Where the Pertinent parameters generated include;

Pressure gradient: $-\frac{\partial \hat{p}}{\partial \hat{x}} = C$

Modified Hartman number: $\frac{l^3 J_0 M_0}{8 \rho \pi^2 v^2} = Hr$

Dust concentration parameter: $\frac{l^2 K_s N_d}{\rho \pi^2 v} = G$

Eckert number: $\frac{v}{C_p (T_2 - T_1)} = Ec$

Magnetic parameter: $\frac{l^3 \sigma B_0^2 \sin^2 \gamma}{v^2 \rho \pi^2} = M$

Prandtl number: $\frac{\rho c_p v}{k_c} = \mathrm{Pr}$

Particle Mass Parameter: $\frac{N_d K_s l^3}{m_d v^2 \pi^3} = S$

International Journal of Recent Research in Mathematics Computer Science and Information Technology
Vol. 11, Issue 2, pp: (84-91), Month: October 2024 – March 2025, Available at: www.paperpublications.org

Permeability parameter: $\frac{\nu l^3}{k_* \pi^2 v^2} = L$

Gravity parameter: $R^* = f \sin\eta$ where $f = \frac{g l^3}{\pi^3 v^2}$

Joule Parameter: $\frac{l^2 \sigma B_0^2 \sin^2\gamma}{\nu\rho C_p \pi^2 (T_2 - T_1)} =$

Temperature relaxation time parameter: $\frac{k_c}{v \rho_m c_s} = \frac{1}{Q}$

Constant of viscosity: $\frac{\nu}{v} = \xi$ (2.0.18)

substituting the above parameters in the equations (2.0.7) and (2.0.8) gives

$$\frac{\partial\Theta}{\partial\hat{t}} = \frac{1}{Pr}\left(\frac{\partial^2\Theta}{\partial\hat{y}^2}\right) + Ec\left(\frac{\partial\hat{u}}{\partial\hat{y}}\right)^2 + \frac{2G}{3Pr}(\Theta - \Theta_d) + J\hat{u} \quad (2.0.19)$$

$$\frac{\partial\Theta_d}{\partial\hat{t}} = \frac{2G(\Theta - \Theta_d)}{3Q} \quad (2.0.20)$$

$$\frac{\partial\hat{u}}{\partial\hat{t}} = C + \xi\frac{\partial^2\hat{u}}{\partial\hat{y}^2} + H_r e^{-y} + R - \hat{u}(M - L) - Gv^{-1}(\hat{u} - \hat{u}_d) \quad (2.0.21)$$

$$\frac{\partial\hat{u}_d}{\partial\hat{t}} = S(\hat{u} - \hat{u}_d) \quad (2.0.22)$$

3. SOLUTION OF THE PROBLEM

To solve the set of equations (2.0.19) and (2.0.20), explicit Finite difference method is used. This is because the method satisfies basic features of consistency, convergence and stability.

The distance between the plates is 2 since the $y_{\min} = -1$ and $y_{\max} = 1$. The horizontal axis (space variable) is sectioned into (N+1) intervals of equal Δy length that is indexed by $j = 0, 1, \ldots . N$ and the vertical axis (time variable) divided into $(M + 1)$ intervals of length Δt indexed by $k = 0, 1, \ldots M$. The computations uses space and time points (j and k). The descretised form of equation (2.0.10) and (2.0.11) to solve for θ and θ_d at each grid point are presented below:

$$\Theta_j^{k+1} = \Delta t\left(\frac{1}{\mathrm{Pr}}\left[\frac{\Theta_{j+1}^k - 2\Theta_j^k + \Theta_{j-1}^k}{\Delta y^2}\right] - Ec\left[\frac{u_j^k - \Theta_{j-1}^k}{\Delta y^2}\right]^2 + \frac{2G}{3\mathrm{Pr}}\left(\Theta_j^k - (\Theta_\mathrm{d})_j^k\right) - J\,\mathrm{u}_j^k\right) + \Theta_j^k \quad (3.0.1)$$

$$\Theta_d^{k+1} = \frac{2G}{3Q}\Delta t\left(\Theta_j^{k+1} - (\Theta_\mathrm{d})_j^k\right) + (\Theta_\mathrm{d})_j^k \quad (3.0.2)$$

$$\mathrm{u}_j^{k+1} = \left[C + \xi\left(\frac{\mathrm{u}_{j+1}^k - 2\mathrm{u}_j^k + \mathrm{u}_{j-1}^k}{\Delta y^2}\right) - R - u_j^k(M + L) + Hre^{-y} - Gv^{-1}\left(\mathrm{u}_j^{k+1} - (\mathrm{u}_\mathrm{d})_j^k\right)\right]\Delta t + \mathrm{u}_j^k \quad (3.0.3)$$

$$(\mathbf{u_d})_j^{k+1} = \boldsymbol{S\Delta t}\left(\mathbf{u}_j^k - (\mathbf{u_d})_j^k\right) + (\mathbf{u_d})_j^k \quad (3.0.4)$$

4. RESULTS AND DISCUSSION

Figure 4.1 illustrates the effect of inclining Riga plates on the temperature profile. As the inclination angle η increases towards 90°, the parameter R also rises, as shown in Table 1, leading to a corresponding increase in temperature, as depicted in Figure 4.1. This behavior can be attributed to the rise in velocity with increasing η, which causes frictional heating. As fluid particles move past each other at higher velocities, the frequency of collisions and energy exchanges intensifies, resulting in a conversion of kinetic energy into thermal energy. This increased molecular activity raises the temperature within the fluid along the flow direction.

ISSN 2350-1022

International Journal of Recent Research in Mathematics Computer Science and Information Technology
Vol. 11, Issue 2, pp: (84-91), Month: October 2024 – March 2025, Available at: www.paperpublications.org

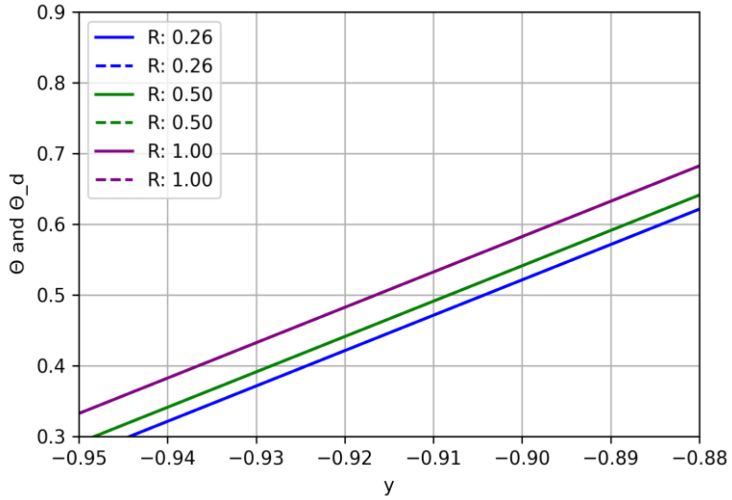

Figure 4.1: Effect of inclining Riga plates on temperature profiles

Table 1: Angle η with corresponding values of R

ANGLE (η^0)	**R=f**$\sin(\eta)^0$
15^0	0.25882
30^0	0.50000
45^0	0.70711
60^0	0.86603
75^0	0.96593
90^0	1.00000

Figure 4.2 demonstrates the effect of an inclined magnetic field on the temperature of the flow. As the dusty fluid moves through the magnetic field, an electric current is induced due to the electromagnetic induction effect. This current encounters resistance within the fluid, leading to Ohmic heating. As the inclination angle γ approaches 90°, the generated current increases, amplifying Ohmic heating and consequently raising the temperature of the fluid. Additionally, Figure 4.2 shows that the temperature of the dust particles, Θ_d, also rises with increasing inclination angle γ. The dust particles interact with fluid particles undergo- ing Ohmic heating, allowing them to absorb heat from the surrounding fluid and, in turn, experience a temperature increase.

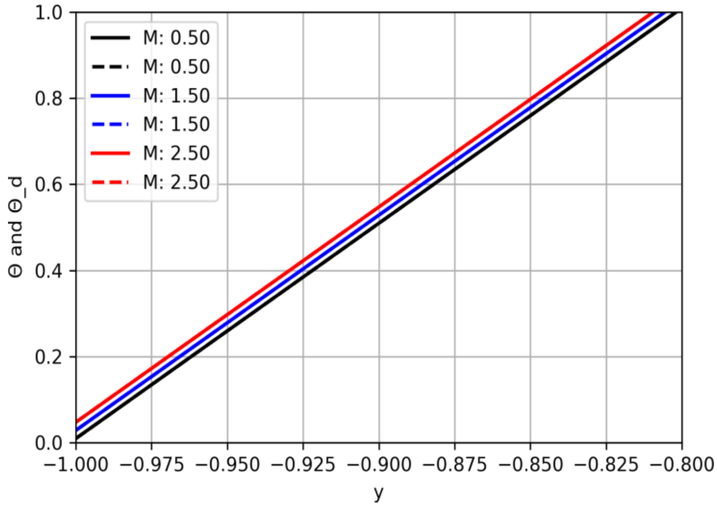

Figure 4.2: Effect of Magnetic Inclination On Θ and Θ_d

Figure 4.3 illustrates a general increase in flow temperature when the dust concentration (G) is increased an observation similarly made by [4]. This observation is attributed to the interactions between dust and fluid particles that lead to additional energy dissipation as heat. The friction and drag forces between fluid and dust particles convert kinetic energy into thermal energy henceforth increasing the temperature and lowering the velocity of the flow.

ISSN 2350-1022

International Journal of Recent Research in Mathematics Computer Science and Information Technology
Vol. 11, Issue 2, pp: (84-91), Month: October 2024 – March 2025, Available at: www.paperpublications.org

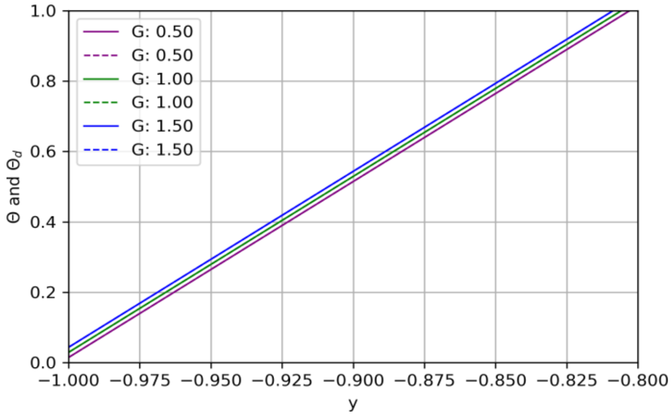

Figure 4.3: Effect of dust particle concentration on temperature profiles

As observed in figure 4.4, there is a general increase in temperature of the flow. As the fluid flows through the channel, an increase in pressure gradient leads to higher flow velocities. The increased velocity results in increased frictional heating where the fluid and dust particles rub against each other and the channel walls hence the increase in flow temperature.

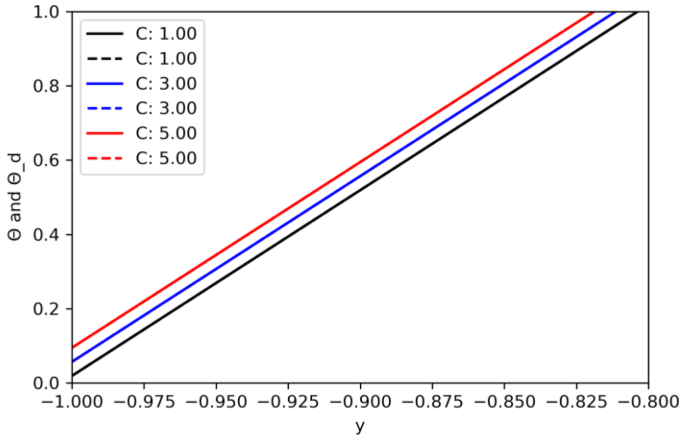

Figure 4.4: Effect of C on u, u_d, Θ and Θ_d

The figure 4.5 presents the results of variation in values of modified Hartman number (H_r) from 0.5 to 1.5. Hartmann number is a dimensionless number defining relationship comparing electromagnetic force and viscous force. The observation show the temperature of both fluid and dust particles increase as modified Hartman number H_r increases. This is caused by the resistance of the fluid to the flow of electrical currents induced by the magnetic field. An increase in the modified Hartmann number increases the electrical currents and, consequently Ohmic heating in the fluid. There is heat transfer through collisions and interactions between the fluid and dust particles, leading to an increase in the temperature of the dust particles.

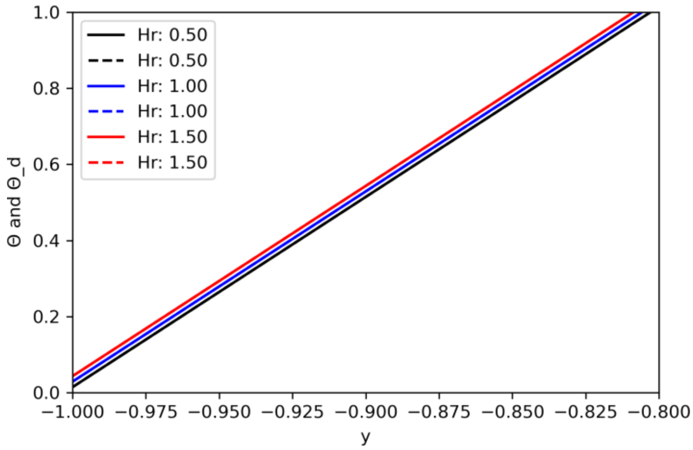

Figure 4.5: Effect of modified Hartman number on u, u_d, Θ and Θ_d

ISSN 2350-1022

International Journal of Recent Research in Mathematics Computer Science and Information Technology
Vol. 11, Issue 2, pp: (84-91), Month: October 2024 – March 2025, Available at: www.paperpublications.org

The temperature of the flow is seen to increase as permeability of the porous medium increases as visualized by figure 4.6. An increase in permeability allows for easier fluid flow through the porous medium. This increased flow rate leads to higher fluid velocities which in turn results in increased frictional heating. As the fluid moves through the porous medium more rapidly, it picks up more heat from the surroundings and transfer it to the dust particles suspended in it.

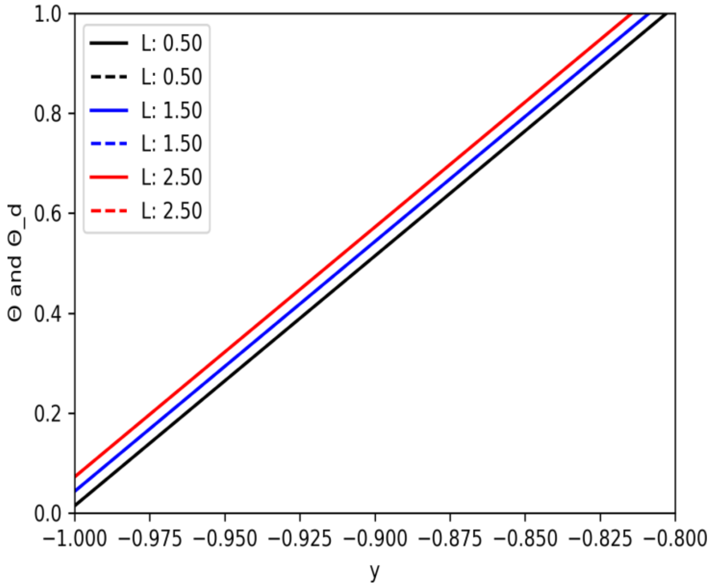

Figure 4.6: Effect of permeability parameter (L) on u, u_d, Θ and $Θ_d$

Eckert number (Ec) is a dimensionless parameter in fluid dynamics and heat transfer that defines the relative importance of kinetic energy compared to heat content. As Eckert number increases as seen in figure 4.7, Kinetic energy of the fluid becomes more significant causing an increase in fluid velocity u. The kinetic energy is converted to thermal energy due to friction and drag forces. This generally increases the temperature of the flow as seen by increase in fluid temperature Θ and dust particles $Θ_d$. As the flow's temperature rises it increases thermal drag on dust particles [1, 6, 9].

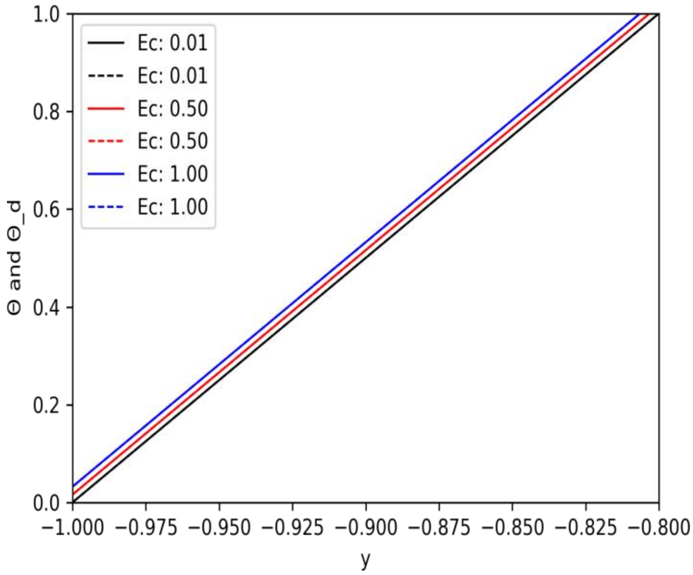

Figure 4.7: Effect of Eckert number on temperature of fluid and dust particles.

Figure 4.8 illustrates that an increment in dimensionless Prandtl parameter results to a slight rise in temperature (Θ and $Θ_d$). Prandtl number relates momentum diffusivity of a fluid to its thermal diffusivity. As Pr increases, it indicates that thermal diffusivity is relatively lower compared to momentum diffusivity. This translates to fluid particles transferring momentum more efficiently than heat hence a general low rise in temperature of the flow.

ISSN 2350-1022

International Journal of Recent Research in Mathematics Computer Science and Information Technology
Vol. 11, Issue 2, pp: (84-91), Month: October 2024 – March 2025, Available at: www.paperpublications.org

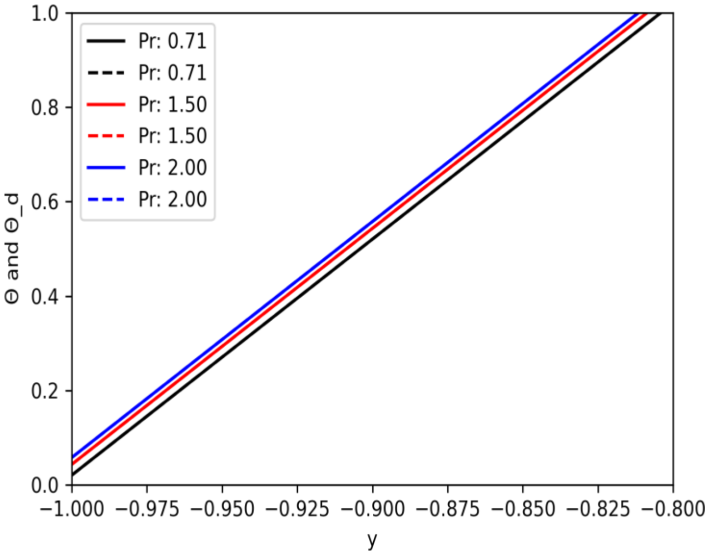

Figure 4.8: Effect of Prandtl number on temperature profiles

5. CONCLUSION

The effects of Riga plates and magnetic field inclination on the temperature profile in the unsteady magnetohydrodynamic (MHD) Stokes flow of a dusty fluid have been analyzed. The system of governing equations was solved using the explicit finite difference method. The results show that the temperature of both the fluid and dust particles increases with rising inclination angle (η), magnetic inclination angle (γ), and dust particle concentration (G). Furthermore, an increase in the pressure gradient (C), modified Hartmann number (H_r), Eckert number (Ec), and Prandtl number (P_r) leads to a corresponding rise in flow temperature.

REFERENCES

[1] Chen, J., Li, Z., and Zhang, X. (2023). Effect of eckert number on thermal drag and particle velocity in dusty fluid flow. *Physics of Fluids*, 35(5):053304.

[2] Iqbal, Z., Azhar, E., Mehmood, Z., and Maraj, E. (2017). Melting heat transport of nanofluidic problem over a riga plate with erratic thickness: Use of keller box scheme. *Results in physics*, 7:3648–3658.

[3] Islam, M. R. and Nasrin, S. (2021). Micropolar fluid flow along with an inclined riga plate through a porous medium. *Int. J. Heat Technol*, 39:1123–1133.

[4] Islama, M. and Nasrinb, S. (2020). Dusty fluid flow past between two parallel riga plates embedded in a porous medium.

[5] Ismail, A. M. and Ganesh, S. (2014). Unsteady stokes flow of dusty fluid between two parallel plates through porous medium. *Applied Mathematical Sciences*, 8(5):241–249.

[6] Kumar, A. and Choi, C. (2022). Thermal drag effects on particle dynamics in high- temperature fluid flows. *Journal of Thermal Science and Engineering Applications*, 14(3):031012.

[7] Onyinkwa, L. M. and Chepkwony, I. (2023). Heat and mass transfer in mhd flow about an inclined porous plate. *Journal of Engineering Research and Reports*, 25(4):106–115.

[8] Otieno, O. R., Manyonge, A. W., and Bitok, J. K. (2017). Similarity transformation analysis of heat and mass transfer effects on steady buoyancy induced mhd free convection flow past an inclined surface. *Journal of Innovative Technology and Education*, 4(1):83–96.

[9] Zhang, L., Wang, H., and Liu, Y. (2021). Influence of temperature gradients on ther- mal drag and particle velocity in dusty fluids. *International Journal of Multiphase Flow*, 137:103680.